**Plant Protection (Scientific Journal of Agriculture)**

**49(2), Summer, 2026**

**10.22055/ppr.2026.52824.1903**

# Characterization of pathogenic fungi associated with decline and root rot of apricot as well as nectarine trees in Semnan Province, Iran

E. Haji-Mohammadi[*1], K. Rahnama[2], Sh. Mojerlou[3]

**1,2. *Corresponding Author:** Department of Plant protection, Gorgan University of Agricultural Sciences and Natural Resources, Golestan, Iran (elahe.mohammadi_s03@gau.ac.ir)

3. Department of plant protection, Shahrood University of Technology, Shahrood, Iran

Received: 30 July2 026 Revised: 5 October 2026 Accepted: 14 October 2026

**Abstract**

Decline caused by pathogenic fungi is an important disease of apricot and nectarine trees in Iran. In this study, root samples were collected from apricot and nectarine trees exhibiting decline symptoms, such as leaf chlorosis, wilting, and dieback. Roots; were surface-sterilized and plated on potato dextrose agar (PDA). Fungal isolates were purified and characterized based on morphological features, particularly asexual spores (microconidia, macroconidia) and sometimes thick-walled, rounded chlamydospores occurring in chains. Eight fungal species were identified based on morphological characteristics. Also, molecular identification was carried out for five of the species through sequencing the ITS1-5.8S-ITS2 region of the nuclear ribosomal DNA. These five species included *Clonostachys rosea*, *Dactylonectria torresensis*, *Fusarium avenaceum*, *F. proliferatum*, and *F. ensiforme*. The other three species, *Fusarium solani*, *F. oxysporum*, and *F. equiseti*, were identified based on unique morphology as well as sufficient sporulation. A total of 53 fungal isolates were obtained, with all isolates subjected to pathogenicity tests on healthy detached branches kept at 25 °C; 18 isolates induced darkening and necrosis of tissues within three weeks and were therefore considered pathogenic. Regarding the lesion length, *Fusarium avenaceum* was the most aggressive species. The five molecularly confirmed species are reported as new records for apricot and nectarine trees in Iran.

***Keywords: Root-infesting fungi, Fruit tree decline, Apricot, Nectarine***

Associate editor: M. Najafiniya (Ph.D.)

**Citation:** Haji-Mohammadi, E., Rahnama, K., & Mojerlou, Sh. (2026). Characterization of pathogenic fungi associated with decline and root rot of apricot as well as nectarine trees in Semnan Province, Iran. *Plant Protection (Scientific Journal of Agriculture), 49*(2), 215-236. https://doi.org/10.22055/ppr.2026.52824.1903

گیاه‌پزشکی (مجله علمی کشاورزی)
جلد ۴۹، شماره ۲، تابستان ۱۴۰۵

10.22055/ppr.2026.52824.1903

# شناسایی قارچ‌های بیماری‌زای مرتبط با زوال و پوسیدگی ریشه درختان زردآلو و شلیل در استان سمنان، ایران

الهه حاجی‌محمدی *[1]، کامران رهنما [2]، شیده موجرلو [3]

او ۲- * **نویسنده مسوول**: گروه گیاه‌پزشکی، دانشگاه علوم کشاورزی و منابع طبیعی گرگان، گرگان، ایران

۳- گروه گیاه‌پزشکی ، دانشگاه صنعتی شاهرود، شاهرود، ایران

تاریخ دریافت: ۱۴۰۵/۰۵/۰۸ تاریخ بازنگری: ۱۴۰۵/۰۷/۱۳ تاریخ پذیرش: ۱۴۰۵/۰۷/۲۲

## چکیده

**زوال ناشی از قارچ‌های بیماری‌زا، یکی از بیماری‌های مهم درختان زردآلو و شلیل در ایران است. در این پژوهش، نمونه‌های ریشه از درختان زردآلو و شلیلِ دارای علائم زوال — از قبیل زردی برگ‌ها (کلروز)، پژمردگی و خشکیدگی سرشاخه‌ها جمع‌آوری شد. ریشه‌ها پس از ضدعفونی سطحی، بر روی محیط کشت سیب‌زمینی-دکستروز-آگار (PDA) کشت شدند. جدایه‌های قارچی خالص‌سازی و بر اساس ویژگی‌های ریخت‌شناختی، به‌ویژه اسپورهای غیرجنسی (میکروکنیدیوم، ماکروکنیدیوم) و در برخی موارد کلامیدوسپورهای گرد با دیواره ضخیم که به‌صورت زنجیره‌ای تشکیل می‌شوند، شناسایی و توصیف شدند. در مجموع هشت گونه قارچی بر اساس ریخت‌شناسی شناسایی شد. همچنین شناسایی مولکولی پنج گونه با تعیین توالی ناحیه ITS1-5.8S-ITS2 از DNA ریبوزومی هسته‌ای برای تأیید تشخیص ریخت‌شناختی انجام شد. این پنج گونه شامل *Clonostachys rosea*، *Dactylonectria torresensis*، *Fusarium avenaceum*، *F. proliferatum* و *F. ensiforme* بودند. سه گونه دیگر، *Fusarium solani*، *F. oxysporum* و *F. equiseti*، بر اساس ریخت‌شناسی منحصربه‌فرد و اسپورزایی کافی شناسایی شدند. در مجموع ۵۳ جدایه قارچی به‌دست آمد و همه جدایه‌ها تحت آزمون بیماری‌زایی روی شاخه‌های بریده سالم در دمای ۲۵ درجه سلسیوس قرار گرفتند؛ ۱۸ جدایه طی سه هفته علائم تیرگی و نکروز بافت‌ها را ایجاد کردند و بنابراین بیماری‌زا در نظر گرفته شدند. بر اساس طول زخم، *Fusarium avenaceum* تهاجمی‌ترین گونه بود. پنج گونه تأییدشده مولکولی به‌عنوان گزارش‌های جدید برای درختان زردآلو و شلیل در ایران گزارش می‌شوند.**

***کلید واژه‌ها: قارچ‌های مهاجم به ریشه، زوال درختان میوه، زردآلو، شلیل***

دبیر تخصصی: دکتر موسی نجفی‌نیا

## Introduction

The stone-fruit trees, which include peach (*Prunus persica* Mill.) and apricot (*Prunus armeniaca* Lam.), are some of the most commercially significant fruits grown in the temperate parts of the world (FAO, 2023). Nectarine (*Prunus persica* var. *nectarina*), which is a smooth-skinned mutation of the peach, has become increasingly significant in the commercial market thanks to the superior aroma and taste of the fruit. In addition, apricots also bear much nutritional and commercial importance and are a good source of carotenoids, phenolics, and vitamins (Čanadanović-Brunet et al., 2013). Iran is one of the largest producers of apricots and nectarines in the world, making the health of the orchards significant aspect.

Root health is essential for the health of the tree, including providing energy, food, and longevity. Soil-borne pathogenic fungi are critical in root damage and root rotting. In Iran, Fusarium solani has been reported as a major causal agent of root and crown rot of hopbush (Dodonaea viscosa) in Khuzestan Province, highlighting the importance of investigating soil-borne fungal pathogens associated with root diseases in Iranian woody plants (Alavani-Pour et al., 2014). Various genera, such as *Fusarium*, *Dactylonectria*, *Cylindrocarpon*, and *Clonostachys* spp., are confirmed to be the key causal organisms of root and stem rot diseases in stone fruit crops globally (Crous et al., 2021). These fungi impact root tissues, resulting in browning of the vascular system, tissue necrosis, and hindrance of nutrient uptake (Agusti-Brisach et al., 2013). Environmental pressures, congestion of the soil, and poor drainage also facilitate tree infection through altering the rhizosphere microbiome to promote pathogen colonization (Kwak & Weller, 2013).

The fungal pathogens consist of flexible eukaryotes that adopt various adaptive mechanisms such as chlamydospore production, endophytic development phases, and soil persistence as saprophytes (Hyde et al., 2020). Nevertheless, morphological identification is not adequate since there are similar phenotypic characteristics among related genera, thus necessitating the use of molecular approaches in species identification (Crous et al., 2015). The sequencing of the internal transcribed spacer (ITS) region of the ribosomal DNA has become the universal barcode of fungi (Schoch et al., 2012; Vu et al., 2019).

In recent times, studies have indicated that novel species of *Fusarium* and *Dactylonectria* pathogens have been discovered as root pathogens of fruit trees within varying climatic regimes, indicating their adaptability and ability to cope with changing conditions (Boughalleb-M'Hamdi et al., 2018). In light of this observation, of importance is the ability of some fusarioid fungi to persist in arid soils under high temperature conditions, prevalent in the semi-arid climate of northeastern Iran. For instance, members of the *Neocosmospora solani* species complex (formerly *Fusarium solani* species complex) and the *Fusarium oxysporum* species complex produce thick-walled chlamydospores which allow them to survive for many years in dry soils with temperatures higher than 30 °C, without the presence of any susceptible host plant (Ploetz, 2015; Gordon, 2017). Such resistance helps maintain these fungi as inoculum sources in rain-fed orchards it keeps them alive as an active population within the rhizosphere of stone fruit trees in drought episodes. Even though there have been several studies on soil fungi in fruit trees, little is known about the diversity and pathogenicity of root fungi in the stone-fruit orchards of Iran.

Thus, this study was designed to detect and characterize pathogenic fungi responsible for root rot and decline symptoms in nectarines and apricots grown

in northeast Iran using both morphological and molecular approaches. Further, pathogenicity tests were outundertaken to verify the involvement of these fungal strains in causing disease. This study provides new knowledge on the occurrence and pathogenicity of root-related fungi of stone fruits.

## Materials & Methods

### Sampling and Isolation

A systematic survey was conducted between February 2022 and August 2023 across eight commercial apricot (*Prunus armeniaca*) orchards and one adjacent nectarine (*Prunus persica* var. *nectarina*) orchard located in Mazaj village, Bastam–Shahroud region, Semnan Province, northeastern Iran (36.6177286° N, 55.3895790° E; elevation ≈ 1,420 m a.s.l.). The area is characterized by a semi-arid climate. Based on regional soil reports from the Shahrood Agricultural and Natural Resources Research Center (Semnan AREEO), the soil texture of the sampled orchards is predominantly sandy loam to loam, with a slightly alkaline pH ranging within7.6 to 8.1 and an electrical conductivity (EC) of 1.8 to 3.2 dS $m^{-1}$ (Shahrood Agricultural Research Center, 2022). A total of 11 symptomatic trees (10 apricot and 1 nectarine), aged approximately 10–15 years, were selected for the sampling. The apricot trees belonged to the dominant local cultivar ‘Shahroudi’, grafted onto myrobalan plum (*Prunus cerasifera*) rootstocks. The nectarine tree was identified as the ‘Independence’ cultivar, grafted onto the GF677 (peach × almond hybrid) rootstock. Trees were selected based on the presence of visible decline symptoms, including lowered vegetative growth, leaf chlorosis, branch dieback, and suspected root rot. From each selected tree, four root samples (each 10–15 cm in length and 0.5–1.5 cm in diameter) were excavated from the upper 30 cm of the rhizosphere. The sampling specifically targeted root sections exhibiting visible symptoms of discoloration, necrosis, or softening. The samples were immediately placed in sterile polyethylene bags, labeled, and transported to the laboratory in a cooled icebox (4 °C) for processing within 24 hours. In order to isolate potential root-associated pathogens, small sections (3–4 cm) were excised above and below the symptomatic root tissue. The middle portion of each sample was surface-sterilized through immersion in 1% sodium hypochlorite for 45 seconds, followed by 70% ethanol for 30 seconds, and rinsed three times in sterile distilled water. Excess moisture was removed with sterile filter paper. Root fragments of approximately 5–10 mm were aseptically transferred onto potato dextrose agar (PDA) for general isolation as well as onto two selective media, synthetic nutrient-poor agar (SNA) and carnation leaf agar (CLA), to recover a broad spectrum of fungal taxa, with emphasis on *Fusarium* (Leslie & Summerella. 2016) .Plates were incubated at 25 ± 1 °C for 5–7 days under dark conditions, with emerging colonies were sub-cultured to fresh PDA plates for purification. In order to ensure long-term maintenance, actively growing cultures were stored on PDA slants at 4 °C and periodically transferred. In recent studies, the use of semi-selective media such as Komada’s medium or PARPH-V8 has been found to ameliorate recovery of *Fusarium*, *Cylindrocarpon/Ilyonectria*, and *Phytophthora* spp. from symptomatic root tissues (Pervaiz et al., 2020; Luo et al., 2022). Further, the combination of traditional culturing and ITS-based molecular diagnostics is now recognized as an essential step for accurate identification of morphologically similar soil-borne fungi (Calle et al., 2024; Hemida et al., 2024). This integrated approach enhances detection reliability and provides a clearer picture of

the fungal community linked to root rot in stone fruit orchards.

**Purification**

Purification of fungal isolates was performed using the single-spore isolation method, a widely used technique for obtaining pure cultures of spore-producing fungi (Zhang et al., 2013; Ma et al., 2022). Sporulating regions of the culture were carefully scraped with the tip of a sterile needle and transferred into a test tube containing 9 mL of sterile distilled water. The suspension was homogenized, with 1 mL of this transferred to another tube containing 9 mL of sterile distilled water to perform serial dilution. The mixture was vortexed to obtain a suitable spore concentration. A drop of the diluted suspension was placed on a hemocytometer slide and inspected under a light microscope to estimate spore density. Dilutions were adjusted to ensure that individual spores were sufficiently separated when plated on the medium surface (Paré et al., 2022).

Next, a few drops of the prepared spore suspension were spread onto Petri dishes containing a thin layer of 2 % water-agar (WA) and incubated at 25 °C to allow spore germination. After 48 h, each plate was carefully examined under a light microscope without opening the lid. Germinated spores that were well-separated from others were marked, whereby the agar blocks containing the germinated spores were transferred using a sterile needle to Petri dishes containing appropriate culture media such as CLA, PDA, and SNA. The plates were then incubated at 25 °C to allow colony development (Yuan et al., 2023).

Recent advances underscore combining classical single-spore isolation techniques with molecular confirmation to enhance identification accuracy, especially for morphologically similar soil-borne pathogens (Zhang et al., 2013; Ma et al., 2022). Also, innovative approaches using super-absorbent polymers and low-cost devices have been found to boost isolation efficiency for arbuscular mycorrhizal and other soil-borne fungi (Paré et al., 2022). This protocol ensures that the isolated cultures are derived from single spores, providing pure material for downstream morphological as well as molecular analyses.

**Pathogenicity Test**

The pathogenicity of fungal isolates was ascertained using a detached-shoot inoculation method, a commonly accepted approach for appraising the virulence of root and trunk pathogens in woody plants (Delgado et al., 2022; Çakar et al., 2025). One-year-old branches of stone-fruit trees (length 20–25 cm, diameter ~1 cm) were selected. Following removal of secondary branches and excess leaves, the branch surfaces were disinfected with 96 % ethanol and then air-dried on sterile filter paper. An oblique slit (~3 cm) was cut in the bark using a scalpel. An 8 mm diameter agar plug carrying active fungal mycelium was inserted under the slit and then covered with parafilm to maintain humidity. The inoculated branches were placed individually in plastic desiccator-type containers with a small amount of sterile distilled water to maintain high humidity, and then incubated at 25 °C. Branch ends were sealed with parafilm to prevent evaporation. For controls, agar plugs without fungal mycelium were utilized.. Each fungal isolate was tested on three branch samples.

Progress of necrotic tissue in bark and underlying wood was monitored, with the lesion length or area measured at appropriate time points (Çakar et al., 2025). To fulfil Robert Koch's postulates, symptomatic tissue segments were re-isolated: after surface disinfection, they were transferred to PDA medium, and examined for recovery of the original fungus (Shen et al., 2024).

**Morphological identification**

The isolates were identified to genus and species through examining the colony characteristics (shape and color) and morphological characteristics such as phialides, macroconidia, microconidia, and chlamydospores, as well as using the identification keys of the isolates. (Barnett & Hunter, 2006; Leslie & Summerella., 2006; Saremi, 2008; Leslie & Summerella., 2016). The Olympus model 51 BX light microscope was applied to describe the pelage, check the microscopic features, and check the morphometric features. A graduated slide and Mosaic 2.2.1 software were employed.

**Molecular identification**

Genomic DNA extraction was performed by the CTAB method. For this purpose, disks of fresh fungus colonies grown on PDA medium were then transferred to a PD-broth liquid culture medium (PD-b). The bottles containing PD-b medium were transferred to the shaker (at a speed of 120 revolutions per minute); after about one week, the fungal mycelium was obtained. After filtering, the mycelium was powdered in a sterile mortar, with 600 microliters of CTAB buffer added to the vials containing the mycelium powder and mixed thoroughly. Next, 2 µl of mercaptoethanol was added to each of the vials, and then they were transferred to a water bath at 65°C. After 45 minutes, for deproteinization, 600 microliters of chloroform-isoamyl alcohol mixture at a ratio of 1:24 was added to each vial and centrifuged for 10 minutes at 12,000 rpm. Following centrifugation, three phases were formed: the lower phase was chloroform, while the upper phase contained DNA. A layer consisting of the cell wall remains was placed between these two liquid phases. The upper phase was carefully transferred to new vials, and the same volume of cold isopropanol was added to the contents of the vials. After inverting the vials ten times, they were kept at -20° for half an hour. Following this period, the tubes were centrifuged for 15 minutes at 13,000 rpm, and eventually, after DNA precipitation, the liquid phase was drained, and the precipitate was washed with 70% ethanol. After drying the DNA precipitate, 70 µl of injected distilled water was added to each vial, and after 30 minutes of storage in the refrigerator, it was transferred to the freezer at -20°. For preparing 100 ml of gel, one gram of agarose powder was boiled in 90 ml of TBE buffer for one minute on a heater, and its final volume was diluted to 100 ml with buffer. After lowering the temperature of the solution to about 50°C, the gel tray was placed inside the mold and combed to create a well on the tray. A 0.5 cm-thick agarose solution was poured into the tray. After closing the gel, the tray was removed from the mold and placed inside the electrophoresis tank. The electrophoresis tank was covered with TBE buffer until the surface of the gel is 1 mm thick. Afterwards, the comb was slowly removed from the gel. Specifically, 5µl of DNA were mixed with 1µl of loading dye and poured into the wells created in the gel. A molecular marker was employed to measure DNA. The electrodes of the tank were connected to the direct current generator, and its voltage was set to 85. ITS4 and ITS5 primers were applied for PCR amplification. Further, 2 µl of primer, 2 µl of genomic DNA, 12.5 µl of master mix, and 8.5µl of double-distilled water were used. Next, sequencing was performed by Pishgam Biotechnology Company using the Sanger (dideoxy chain-termination) method. The obtained genome sequence was analyzed through BLAST software in NCBI, and its similarity with other sequences available in the World Bank was determined. Axes were drawn via MEGA 11 software (Guerra et al., 2020).

## Results

**Field symptoms**

Field surveys conducted between February 2022 and August 2023 in eight

apricot orchards and one nectarine orchard in the Bastam–Shahroud region, Semnan Province, revealed characteristic decline symptoms in affected trees. The observed symptoms included reduced vegetative growth, leaf chlorosis (Figure 1e), wilting and progressive dieback of branches (Figures 1b, 1c, and 1d), gum exudation from the trunk (Figure 1a), and dark brown to black vascular discoloration in cross-sections of branches and crown tissues (Figure 1f). These symptoms are indicative of vascular dysfunction and root necrosis, commonly associated with root-infecting fungal pathogens. The severity of symptoms was more pronounced in older orchards and those managed under traditional practices with poor drainage and deep planting of graft unions; however, due to the qualitative nature of these observations, statistical analysis was not performed.




**Figure 1. Deterioration symptoms on stone fruit trees: a. Gum secretion from the trunk of the apricot tree; b. The drying of the apricot trees, c, d- The drying of blossoms and leaves of apricot trees; e. Yellowing of the leaves of the nectarine tree; f- The spread of dark-colored signs in the cross-section of the branches of circular and sectored tree branches**

**Frequency and distribution of fungal species**

From symptomatic root and crown tissues, a total of 53 fungal isolates were obtained. Following pathogenicity tests on detached shoots, 18 isolates induced vascular necrosis and tissue darkening and were confirmed as pathogenic. These 18 pathogenic isolates were identified as eight distinct species based on morphological characteristics and, for five species, molecular confirmation. Among the pathogenic isolates, *Fusarium oxysporum* and *Fusarium solani* were the most frequent species, each represented by 4 isolates (22.2% of the pathogenic isolates), followed by *Clonostachys rosea* with 3 isolates (16.7%). *Fusarium avenaceum* and *Fusarium equiseti* each comprised 2 isolates (11.1%), while *Fusarium proliferatum*, *Fusarium ensiforme*, and *Dactylonectria torresensis* were each represented by a single isolate (5.6% each). Three species—*F. solani*, *F. oxysporum*, and *F. equiseti*—were identified solely by morphological features due to their distinctive sporulation, whereas the remaining five species were confirmed by molecular identification (ITS sequencing).

***Fusarium avenaceum*: (Fr.) Sacc., Syll. Fung. 4: 713. 1886. Basionym: *Fusisporium avenaceum* Fr., Syst. Mycol. 2: 238. 1822, nom. sanct. [Fr., l.c.]**

The diameter of the fungus colony after 3 days on potato-dextrose-agar medium at 25±1°C was 4.2 cm. The upper surface of the mycelia was dark red (Figure 10-a). The sickle-shaped macroconidia and their dorsal and ventral walls are parallel in the middle, and they look needle-shaped (Figure 2-b). Macroconidia are formed on single phialides and on branched conidiophores in sporodochiums, which have 3 or 4 transverse walls, and their dimensions are on average (2.34-2.01) 3.86 x (35.26) 23.82) 31.73 micrometers. Egg-shaped microconidia with dimensions (3.06-5.78) 3.67 x (9.17-14.37) 11.46 micrometers were formed in CLA medium (Figure 2-a).

Chlamydospores are absent in this species. The characteristics of these isolates were consistent with the descriptions mentioned by Leslie & Summerella (2006) and Saremi (2008). The results of the molecular studies also showed that isolate 8a belongs to this species, and according to the gene tree, the isolate was placed in the same clade with *Fusarium avenaceum* species (Figure 12).

***Fusarium proliferatum:* (Matsush.) Nirenberg ex Gerlach & Nirenberg, Mitt. Biol. Bundesanst Land- Forstw. 209: 309. 1982**

After 3 days on potato-dextrose-agar medium at a temperature of 25±1°C, the diameter of the fungus was 4.3 cm. The top surface is white, and the back surface produces yellow pigments(Figure 10-b). Long, sickle-shaped, and mostly elongated macroconidia with 3 to 5 transverse walls with dimensions of (4.98-3.37) 4.26 x (25.66-37.61) 31.40 micrometers on CLA medium. Macroconidia were produced from single phialides and branched conidiophores (Figure 3-b, 3-c). Egg-shaped microconidia with dimensions (1.46-2.99) 2.32 x (5.68-10.10) 15.8 micrometers in chains on branched phialides, mostly in pairs and V-shaped. (Figure 3-a). There were no chlamydospores in this species. Also, the results of molecular work showed that isolate 13c belongs to this species, and by drawing the gene tree, the isolate was placed in a clade with *Fusarium proliferatum* species (Figure 12).

***Fusarium ensiforme:* Wollenw. & Reinking, Phytopathology 15: 169. 1925**

After 3 days of incubation on potato dextrose agar (PDA) at 25 ± 1 °C, the diameter of the fungus was 3.1 cm. The colony surface was white, and orange pigments were produced with increasing colony age (Figure 10-c). Conidiophores were simple or branched, reaching up to 100

µm long and 3.5–6.5 µm wide at the base. Phialides were cylindrical to subcylindrical (Figure 4-a). Macroconidia were hyaline, falcate, and dorsiventrally curved, mostly with 3 transverse septa, measuring (27–44) 34 × (4–6.4) 5.3 µm. Four-septate macroconidia measured (36–40) 38 × (5.7–6.2) 5.95 µm (Figure 4-b). Microconidia were oval to elongated-oval, occasionally clavate, and mostly aseptate or 1-septate. Aseptate microconidia measured (3.6–11.5) 7.58 × (2.8–6.3) 4.8 µm, whereas 1-septate microconidia measured (10–23) 13.5 × (4–6.0) 4.8 µm. Chlamydospores were relatively abundant, globose to subglobose, terminal or intercalary, measuring 8–15 µm in diameter. They occurred singly, in clusters, or in short chains (Figure 4-c). The results of molecular analysis also showed that isolate 8e belongs to *Fusarium ensiforme*, and phylogenetic analysis showed that the isolate was placed in the same clade with reference isolates of *F. ensiforme* (Figure 12).

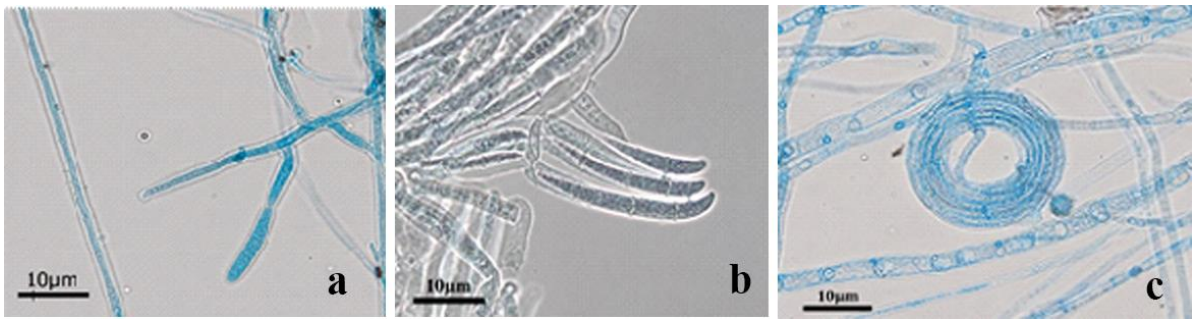



**Figure 2. Microscopic characteristics of the fungus *Fusarium avenaceum* (Gau, 8a): a. microconidia in natural media culture on CLA; b. macroconidia; c. torus hyphae**

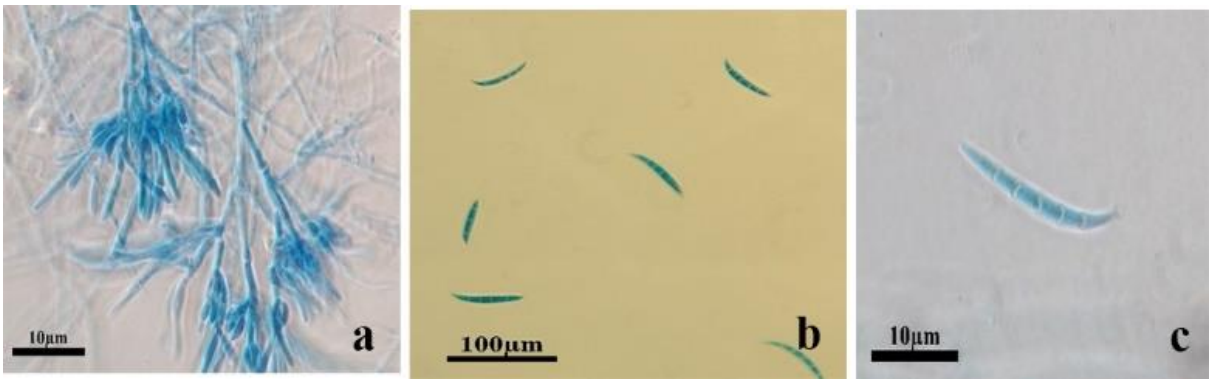



**Figure 3. Microscopic characteristics of the fungus *Fusarium proliferatum* (Gau,13c): *a.* Microconidia under natural conditions on CLA; b. macroconidia; c. macroconidia**

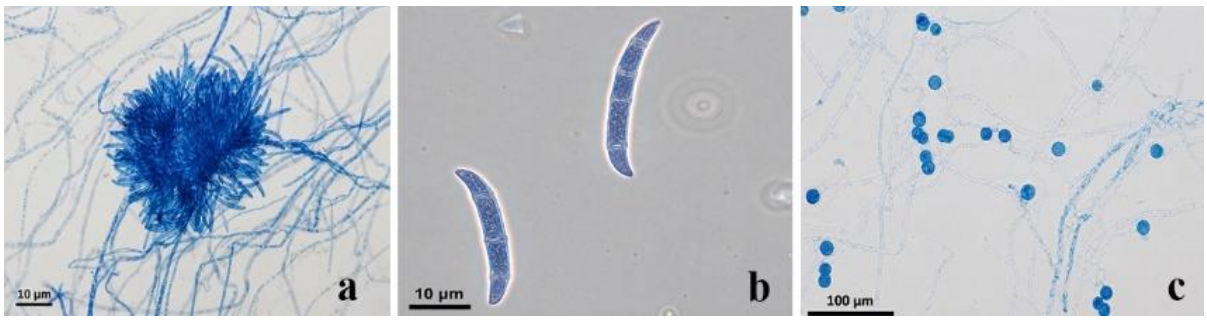



**Figure 4. Microscopic characteristics of the fungus *Fusarium ensiforme* (Gau, 8e): a. Microconidia under natural conditions on CLA; b. Macroconidia; c. Chlamydospores**

***Fusarium oxysporum:*** **Schltdl., Fl. Berol. 2: 139. 1824**

The diameter of the fungus colony after 3 days on potato-dextrose-agar medium at 25±1°C was 3.25 cm. It has cottony mycelium and scattered and dense white hyphae, which produced orange pigments in some isolates (Figure 10-e). The macroconidia were boat-shaped and led to a point on both sides and were produced on single phialides or branched conidiophores in the sporoduchium. They also had 3 or 4 transverse walls with dimensions of (2.15-2.95) 2.59 x (16.98-47.32) 29.44 micrometers (Figures 5-b). Microconidia are usually single-celled, ovoid, or ovoid, with dimensions of (1.95-3-90) 3.002 x (11.68-16-70) 13.74 micrometers. They were formed on short single phialides (Figure 5-a). Also, terminal single-cell chlamydospores and some two-cell chlamydospores were formed on CLA medium (Figure 5-c).

***Fusarium equiseti:*** **(Corda) Sacc., Syll. Fung. 4: 707. 1886**

The diameter of the colony after 3 days on potato-dextrose-agar medium at 25°C was 3.3 cm. This species produced dense and uniform white to light brown mycelia. The color of the colony on the back of the petri dish was light brown (Figure 10-f). Macroconidia are strongly curved and have 5 to 7 transverse walls with the dimensions of (2.50-4.85) 3.43 x (44.28) - 28/64) 37/19 on the SNA culture medium. The terminal cell is elongated and ends at a point, and the basal cell is observed as a heel (Figure 6-a, c). Microconidia are not formed in this species, but they produce chain or cluster chlamydospores measuring 10.50 x 16.46 micrometers.

***Fusarium solani*****: (Mart.) Sacc., Michelia 2: 296. 1881**

***Neocosmospora solani*** **(Mart.) L. Lombard & Crous, Stud. Mycol. 80: 228. 2015**

The diameter of the fungus colony after 3 days on potato-dextrose-agar medium at 25±1°C was 3.38 cm. It produced white to cream-colored mycelium in a scattered and cottony form (Figure 10-h). The macroconidia were generally sausage-shaped, and their diameter and width were large, with 3 or 4 transverse walls with dimensions of (4.30-5.07) 4.69 x (26.37-38.61) 11.32 micrometers. They were formed on CLA culture medium (Figure 7- a, c). Macroconidia were formed from individual phialides of branched conidiophores on the sporodocium (Figure 7b). The microconidia are one- or two-celled, ovoid, and oval or small-shaped and have dimensions of (3.43-3.74) 3.29 x (9.46-16.45) 13.36 micrometers on phialides. They were observed individually. In recent years, this compound species has been separated and proposed into several genera. One or two-cell chlamydospores were formed at the end with dimensions of 6.32-10.62 by 8.74 micrometers.




**Figure 5. Microscopic characteristics of the fungus *Fusarium oxysporum*: a. Microconidia under natural conditions on CLA; b. macroconidia; c. Chlamydospore**

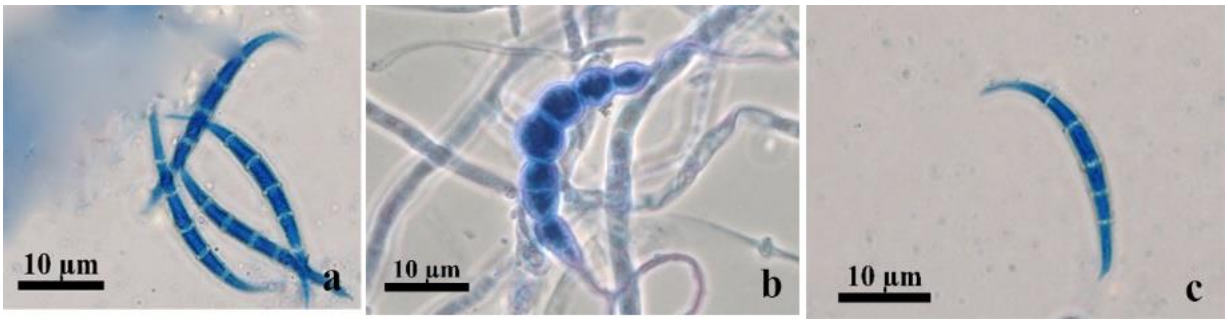



**Figure 6. Microscopic characteristics of *Fusarium equiseti*: a. macroconidia; b. Chlamydospore; c. macroconidia**

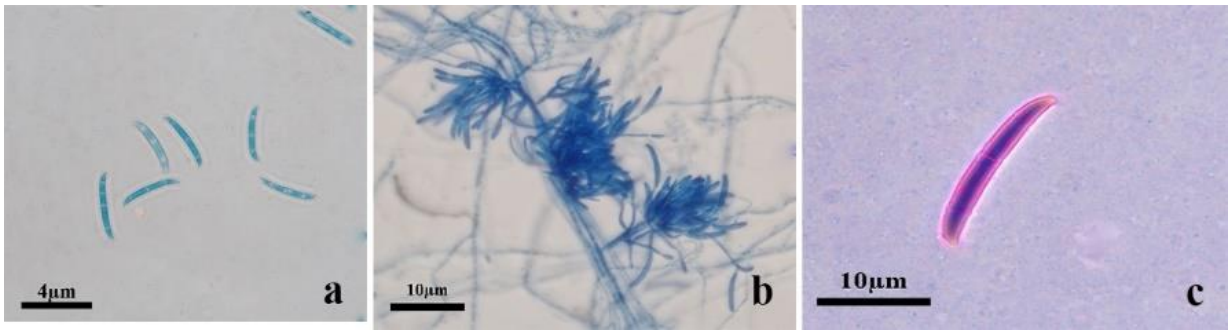



**Figure 7. Microscopic characteristics of *Fusarium solani*: a. macroconidia; b. Sporodochium; c. macroconidia**

***Dactylonectria torresensis*: (A. Cabral, Rego & Crous) L. Lombard & Crous, 2014**

The diameter of the fungus colony after 3 days on potato-dextrose-agar medium at 25±1°C was 2.5 cm. The top surface was orange with a yellowish border, and the back surface was orange-red (Figure 10-g). Macroconidia are cylindrical with 1-3 transverse walls, and their dimensions are on average (5.60- 9.03) 7.46 × (44.28- 58.25) 52.46 micrometers. One-celled microconidia with dimensions of (2.5- 45.57) 3.52 × (12.22- 54.91) 19.44 micrometers were seen on single phialides on CLA medium (Figure 8a, b, c). Also, the results of the molecular investigation showed that isolate 8b belongs to this species, and by drawing the gene tree, the isolate in question was placed in the same clade with *Dactylonectria torresensis* species (Figure 12).

***Clonostachys rosea:* (Link) Schroers, (1999)**

After 3 days of incubation on potato dextrose agar (PDA) at 25 ± 1 °C, the diameter of the fungus was 1.8 cm. The colony surface was covered with white mycelium and produced yellow pigments (Figure 10-d). Conidiophores were dimorphic, consisting of primary verticillate and secondary penicillate conidiophores. The primary conidiophores bore divergent phialides arranged in whorls, measuring (20.5–40.5) × (1.5–3) µm, with stipes measuring 20–122 µm long. The secondary conidiophores were bi- to quaterverticillate and bore adpressed phialides arranged in whorls, measuring (10–19) × (1–3) µm. Conidia were hyaline, smooth-walled, aseptate, cylindrical to ellipsoidal, and slightly curved, measuring (4–10) × (1.5–3.5) µm (Figure 9-a–c). Molecular analysis also showed that isolate 7a belonged to *Clonostachys rosea*, and phylogenetic analysis revealed that the isolate clustered with reference isolates of *C. rosea* in the same clade (Figure 12).

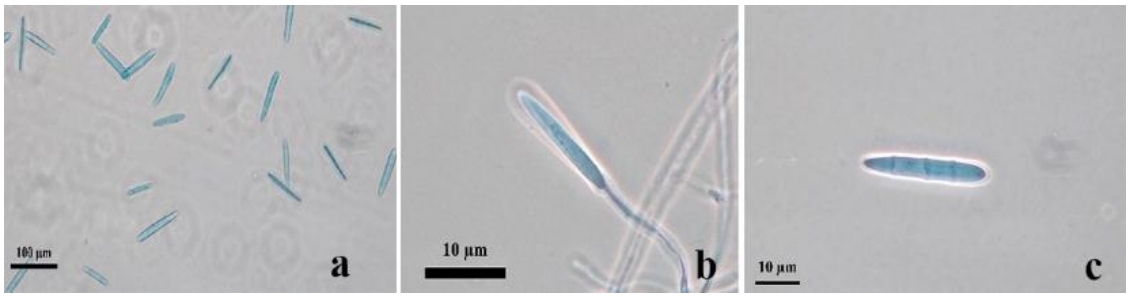



**Figure 8. Microscopic characteristics of *Dactylonectria torresensis*(Gau, 8b) species: a, b, c. macroconidia**

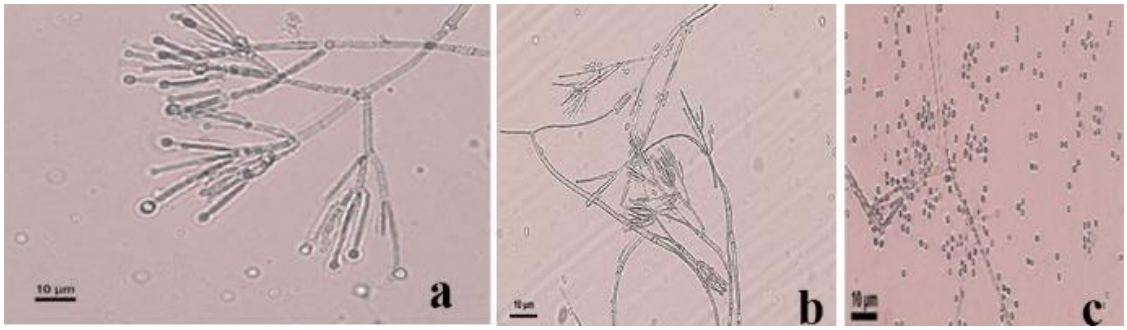



**Figure 9. Microscopic characteristics of the fungus *Clonostachys rosea* (Gau, 7a): a. Primary verticillate conidiophores with divergent phialides; b. Secondary penicillate conidiophores with adpressed phialides; c. Hyaline, aseptate conidia**

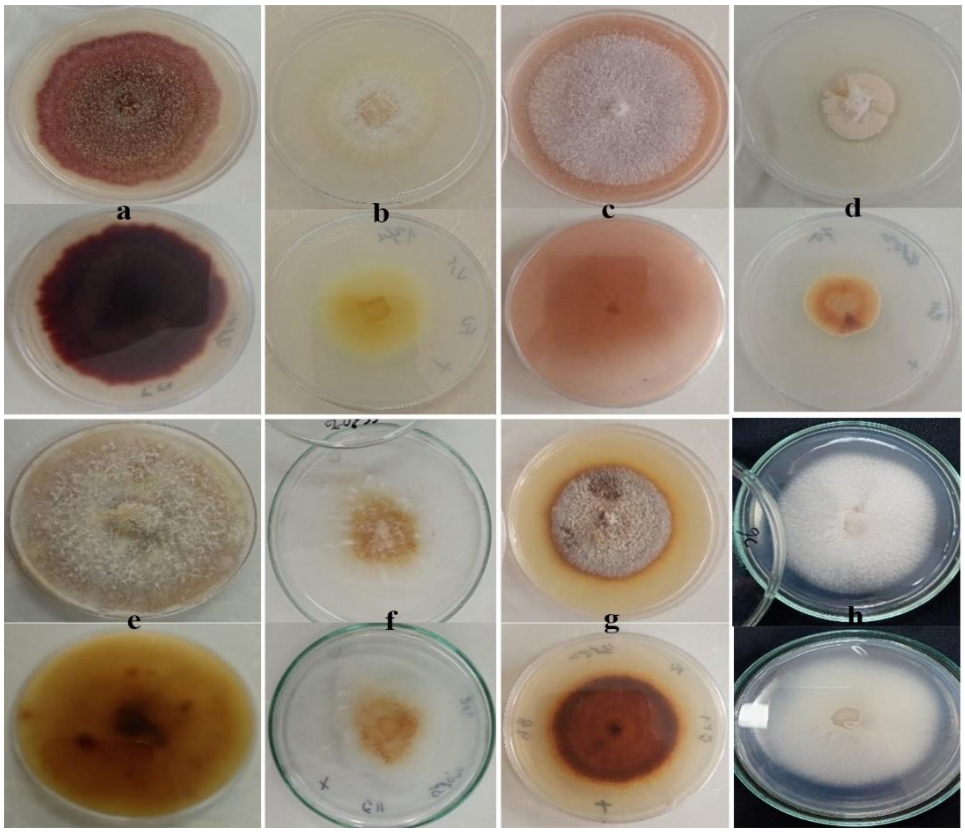



**Figure 10. The top and back surface of the fungus on the PDA culture medium after 7 days (small letters show details); a. *Fusarium avenaceum*, b. *Fusarium proliferatum*, c. *Fusarium ensiforme*, d. *Clonostachys rosea*, e. *Fusarium oxysporum*, f. *Fusarium equiseti*, g. The species *Dactylonectria torresensis*, h. *Fusarium solani***

Pathogenicity tests on detached branches revealed significant differences in lesion length among the tested fungal isolates at the 1% probability level. *Fusarium avenaceum* caused the largest lesions, followed by *F. oxysporum* and *F. solani*. *F. proliferatum* and F. *equiseti* showed moderate to low pathogenicity, while *F. ensiforme* and *Dactylonectria torresensis* caused moderate lesions. *Clonostachys rosea* isolates exhibited only limited necrosis, indicating weak pathogenicity under the tested conditions.

**Phylogenetic analyses**

For molecular phylogenetic analyses, the internal transcribed spacer (ITS) region of the rDNA was amplified and sequenced. All sequences obtained in this study, as well as the reference sequences downloaded from the NCBI GenBank website, were aligned using MAFFT version 7.490 (Katoh & Standley, 2013). The resulting alignment was manually adjusted in BioEdit version 7.2 (Hall, 1999). The ambiguous regions were then removed with trimAl version 1.4 using the gappyout option (Capella-Gutiérrez et al., 2009). The final alignment contained 630 bp-long sequences.

The phylogenetic tree was constructed using the Maximum Likelihood (ML) algorithm implemented in MEGA software version 11 (Tamura et al., 2021). The best-fitting nucleotide substitution model was selected according to the Akaike Information Criterion (AIC) using jModelTest version 2 (Darriba et al., 2012). The Kimura 2-parameter model with gamma distribution (K2+G) was used for ML analysis.

The support of individual branches was estimated with 1,000 bootstrap replicates (Felsenstein, 1985). The bootstrap values are indicated at the nodes. Here, the values from 5 to 100% are shown. All sequences were retrieved using BLASTn and taxonomic studies by other researchers. The representative species of the genera *Fusarium*, *Clonostachys*, and *Dactylonectria* were included, as indicated in the phylogenetic tree below.

The outgroup used for tree rooting was *Biscogniauxia atropunctata* (AY951673.1). This species was selected because it belongs to a different family (*Xylariaceae*) that is related to the remaining species on the tree. In particular, this species was used to root the tree because it is distantly related to the *Nectriaceae* and *Bionectriaceae* families. but still close enough to infer ancestral states of characters. The final tree was plotted with FigTree version 1.4.4.

In order to verify the taxonomic classification of the isolates, the ITS sequences of five isolates (Gau,7a, Gau,8a, Gau,8b, Gau,8e, and Gau,13c) were aligned pairwise against their closest homologous reference sequences found in the NCBI database, which was also used for the generation of the phylogenetic tree (Figure 12). According to the pairwise identity matrix (Figure 12), three out of the five isolates (Gau,8b (*D. torresensis*), Gau,13c (*F. proliferatum*), and Gau,7a (*C. rosea*)) showed 100% identity to their respective reference strains MG685812.1, OQ923669.1, and MH259861.1. Additionally, the isolate associated with *F. ensiforme* (Gau,8e) showed 99.87% identity to LT746247.1, and the isolate related to *F. avenaceum* (Gau,8a) showed 99.93% identity to MT975267.

**Table 1. Analysis of variance (ANOVA) for the effect of fungal isolates on lesion length in detached branch pathogenicity assays**

| Source of Variation | Degrees of Freedom (df) | Mean Square of Lesion Length ($cm^2$) |
|---|---|---|
| Treatment (Isolate) | 17 | 38.13** |
| Error | 36 | 0.05 |
| Coefficient of Variation (CV %) | | 5.34 |

*P*<0.01 (highly significant); ** Significant at the 1% probability level.

**Table 2. Mean comparison of lesion length (cm) caused by different fungal isolates on detached branches**

| Fungal isolate | Lesion length (cm)* | Fungal isolate | Lesion length (cm)* |
|---|---|---|---|
| *F. avenaceum* 8a | 13.66[a] | *F. avenaceum* 9d | 12.50[b] |
| *F. oxysporum* 3c | 5.40[c] | *F. oxysporum* 15ph | 5.40[c] |
| *F. oxysporum* 15a | 5.03[cd] | *F. solani* 3d | 4.73[de] |
| *F. ensiforme* 8e | 4.43[ef] | *F. solani* 14d | 4.33[fg] |
| *F. oxysporum* 15d | 4.33[fg] | *F. solani* 14c | 4.10[fg] |
| *F. solani* 9c | 4.00[g] | *D. torresensis* 8b | 3.56[h] |
| *F. proliferatum* 13c | 3.40[h] | *F. equiseti* 13b | 2.93[i] |
| *F. equiseti* 10e | 2.86[i] | *C. rosea* 7a | 0.23[j] |
| *C. rosea* 7b | 0.00[j] | *C. rosea* 7c | 0.00[j] |

**LSD (Least Significant Difference) = 0.39**
Values are means of lesion length (cm). Means followed by the same lowercase letter are not significantly different according to the LSD test ($P \leq 0.05$).

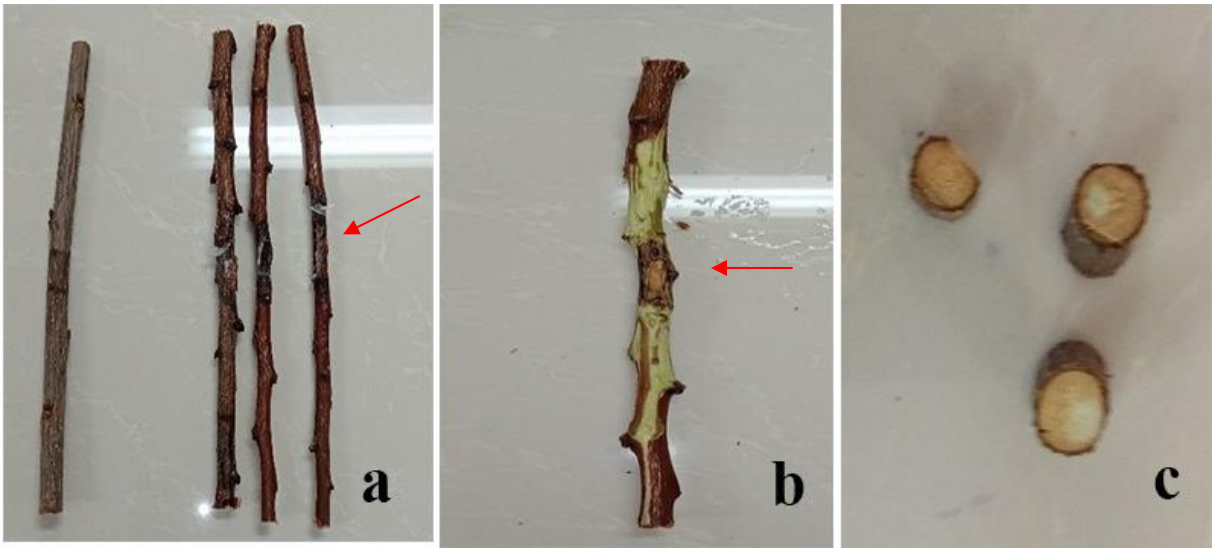



**Figure 11. Symptoms of the disease caused by *Fusarium avenaceum* (Gau, 8a) fungus on cut branches; a. The presence of a dark spot (from the right side of the apricot branches compared to the control without fungus (left); b. The presence of a dark spot on the apricot branch; c. Transverse section of an infected sample of an apricot branch**

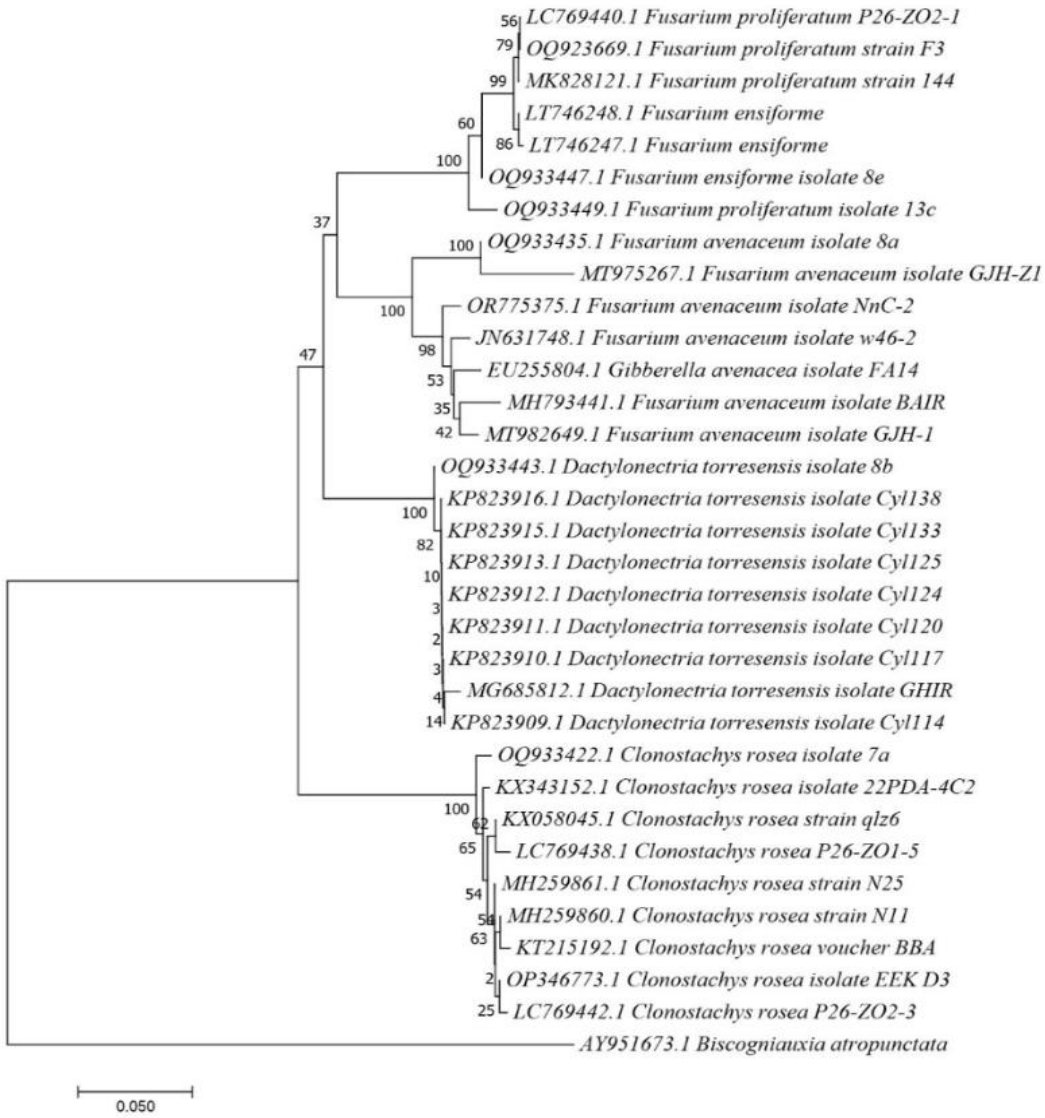



**Figure 12. The gene tree of *D. torresensis* (8b), *F. ensiforme* (8e), *F. proliferatum* (13c), *F. avenaceum* (8a), and *C. rosea* (7a) derived from the ITS gene region using Mega11 software. *Biscogniauxia atropunctata* species is considered a foreign array. The examined fungi (except *C. rosea*, which is in the *Bionectriaceae* family). All of the species were from *the Nectriaceae* family, *Hypocreales* order, class *Sordariomycetes*, and *Ascomycota* phylum**

## Discussion

This paper dealt with a new evaluation of fungal pathogens linked to roots and crowns of apricots (*Prunus armeniaca* Lam.) and nectarines (*Prunus persica* var. *nucipersica*) growing in northeastern Iran. It was found shown that fungi of the genus Fusarium belong to the main fungal groups causing root and crown symptoms. This result is in accordance with those reported in previous and current studies performed in Iran and elsewhere that recognized Fusarium spp. as stable and dominant pathogens of fruit trees (Sabahi et al., 2023; Esmaeili et al., 2024).

The ecological significance of the above observations is noteworthy. The *Fusarium* species have the ability to survive in soils for extended durations through developing chlamydospores and other resistant stages, allowing for their persistence in soil even when there are no available susceptible hosts (Sabahi et al., 2023). Once they are

established, these *Fusarium* species will serve as a source of chronic inocula that lead to orchard decline syndromes.

In addition to *F. solani*, *F. oxysporum*, and *F. equiseti* isolated from the roots as well as crown of peach and nectarine in the same location, Zakeri and Zare (2013) reported other *Fusarium* species by applying a morphology-based survey. Nevertheless, their study was not supported by molecular analysis and did not cover other genera except for *Fusarium* species. In contrast, the current study has been based on an integrated morphological and molecular examination, with sequencing of the ITS region of DNA as a molecular tool. Also, the range of the host plant expanded to cover nectarine and apricot trees. The genus *Dactylonectria* was recorded for the first time in this area. The pathogenicity tests also confirmed that the isolates obtained in the current study would cause root decline. The comparison of the results of the current research and Zakeri and Zare (2013) suggests that the variety of pathogenic species and genera in the last decade has increased, with more adaptable taxa. This re-assessment highlights the significance of conducting periodic studies because of climate changes on root pathogen populations to achieve the appropriate disease control program in stone fruit orchards in this area.

In the present study, about 56% of the isolates obtained belonged to *Fusarium*, implying that despite the last two decades of climate change, *Fusarium* remains the dominant soil-borne pathogen in the region. These fungi were first reported from northeastern Iran by Ershad (2022).

It is crucial to note, however, that the ITS1-5.8S-ITS2 region employed in this research does not yield adequate diversification to identify species belonging to several *Fusarium* species complexes. Even though the ITS region is generally regarded as an excellent fungal barcode owing to the presence of conserved primer binding sites, high copy number, and suitability for genus assignment, its effectiveness in species-level identification is restricted by its low sequence variation among closely related species as well as its intragenomic variability. Hence, the inclusion of protein-coding loci like translation elongation factor 1-α (TEF1) is recommended for species-level identification in the future (Schoch et al., 2012; O'Donnell et al., 2015).

Considering the persistent occurrence of *Fusarium* spp., it becomes essential to implement preventive management methods and the practices of integrated soil health. Some examples of preventive measures include selecting resistant or tolerant rootstocks, enhancing soil ventilation and drainage, and performing continuous nutrition of the tree, which is of paramount importance (Martino et al., 2025).

The weak pathogenicity observed in some *Clonostachys rosea* isolates on detached branches in the present study may reflect the ability of certain strains to shift from an endophytic or saprophytic lifestyle to an opportunistic pathogenic phase under specific conditions. Such lifestyle transitions are well documented in several fungal taxa, where environmental cues, host physiological status, and genetic background can impact the expression of virulence-related traits (Redman et al., 2001; Rai & Agarkar, 2016; Brader et al., 2017). Although *C. rosea* is predominantly recognized as a mycoparasite and biocontrol agent (Sutton et al., 1997; Sun et al., 2020), its occasional recovery from symptomatic tissues as well as weak pathogenic reactions suggest that some isolates may possess opportunistic

pathogenic potential. Nevertheless, the molecular and ecological mechanisms underlying such behavioral plasticity in *C. rosea* remain poorly understood and warrant further investigation.

Methodologically, the pathogenicity tests described in this study were undertaken on detached shoots and not on the organ they derived from – the root system. Detached shoot assays cannot fully replicate the conditions in vivo that are found in living roots (e.g., root-specific defense responses, root wound healing, vascularization, rhizosphere microorganisms, etc.) and can lead to an over- or underestimation of pathogenesis potential. Nevertheless, it is justifiable in terms of this current study (Haji Mohammadi, 2023).

The genera identified (*Fusarium*, *Dactylonectria*, *Clonostachys*) belong to soil-dwelling vascular fungi and can infect as well as colonize throughout the cortical tissues and within the xylem.

The host-pathogen system can only be interpreted as initial root infection results in subsequent spread within the above-ground vasculature, and as such, the inoculation onto stem or shoot segments is commonly employed in initial screening for pathogenesis. Three weeks following inoculation of detached shoots (under controlled conditions), consistent fungal spread was clearly exhibited, revealing vascular discoloration and necrosis as observed. To address the limitation fully, by fulfilling Koch's postulates on the host organ in question, inoculations onto roots would be necessary, and to achieve this, potting of seedlings would be necessary for such tests.

Future research should target: (i) prolonged study of the diversity of *Fusarium* species in relation to climatic conditions, and (ii) simulation of disease risk with the help of modeling based on the climate forecast (Nnadi et al., 2021; Houshyar et al., 2025).

**Concluding Remarks**

In conclusion, the present study revealed that *Fusarium* spp. are significant soilborne pathogens linked with root and crown rot in apricot and nectarine orchards in the Shahrood area of Semnan Province in northeast Iran. The findings underscore the need for the integration of pathogen identification and disease management practices in stone fruit orchards in this geographic area. The comprehensive description of disease symptoms (Figures 1–4) serves as a useful diagnostic tool that can help orchard managers, extension workers, and plant pathologists in the management of similar diseases in other areas with the same agro-ecological conditions. In addition, future surveys should be conducted in other stone fruit-growing regions of Iran to determine a broader distribution and importance of these pathogens.

**Acknowledgments**

The authors gratefully acknowledge Shahrood University of Technology for providing the facilities necessary for sample processing and fungal isolation and purification. They also thank the orchard owners for granting permission to collect samples from their orchards.

**References**

Agustí-Brisach, C., Gramaje, D., García-Jiménez, J., and Armengol, J. 2013. Detection of black-foot disease pathogens in the grapevine nursery propagation process in Spain. *European Journal of Plant Pathology*, *137*, 103–112. https://doi.org/10.1007/s10658-013-0221-8

Alavani-Pour, H., Farokhi-Nejad, R., and Charm, M. 2014. Effects of pH, chelating agents and calcium on root and crown rot of hopbush caused by *Fusarium solani*. *Plant Protection (Iran)*, *37*(3), 113–122.

Barnett, H. L., and Hunter, B. B. 2006. *Illustrated Genera of Imperfect Fungi (Mitosporic Fungi)*. Burgess Publishing Company.

Brader, G., Compant, S., Vescio, K., Mitter, B., Trognitz, F., Ma, L. J., and Sessitsch, A. 2017. Ecology and genomic insights into plant-pathogenic and plant-nonpathogenic endophytes. *Annual Review of Phytopathology*, *55*, 61–83. https://doi.org/10.1146/annurev-phyto-080516-035641

Calle, A., Adelberg, J., Schnabel, G., Naylor-Adelberg, J., Gelain, J., Karakoc, Y., and Gasic, K. 2024. In vitro co-culture system for investigating *Armillaria mellea* root rot in *Prunus* spp. using a fiber-supported liquid approach. *PLOS ONE*, *19*, e0310314. https://doi.org/10.1371/journal.pone.0310314

Capella-Gutiérrez, S., Silla-Martínez, J. M., and Gabaldón, T. 2009. trimAl: A tool for automated alignment trimming in large-scale phylogenetic analyses. *Bioinformatics*, *25*, 1972–1973. https://doi.org/10.1093/bioinformatics/btp348

Čanadanović-Brunet, J. M., Vulić, J. J., Ćetković, G. S., Đilas, S. M., and Tumbas-Šaponjac, V. T. 2013. Bioactive compounds and antioxidant properties of dried apricot. *Acta Periodica Technologica*, *44*, 193–205. https://doi.org/10.2298/APT1344193C

Çakar, D., Akyüz, B., and Şimşek, S. A. 2025. Pathogenicity assessment of *Gnomoniopsis castaneae* on nut and bark tissues of chestnut cultivars in Türkiye. *European Journal of Plant Pathology*, *173*, 223–233. https://doi.org/10.1007/s10658-025-03093-2

Chehri, K., Salleh, B., Yli-Mattila, T., Reddy, K. R. N., and Abbasi, S. 2011. Molecular characterization of pathogenic *Fusarium* species in cucurbit plants from Kermanshah province, Iran. *Saudi Journal of Biological Sciences*, *18*, 341–351. https://doi.org/10.1016/j.sjbs.2011.01.007

Crous, P. W., Lombard, L., Sandoval-Denis, M., and Seifert, K. A. 2021. *Fusarium*: More than a node or a foot-shaped basal cell. *Studies in Mycology*, *98*, 100116. https://doi.org/10.1016/j.simyco.2021.100116

Crous, P. W., Wingfield, M. J., Guarro, J., Hernández-Restrepo, M., Sutton, D. A., Acharya, K., and Dutta, A. K. 2015. Fungal Planet description sheets: 320–370. *Persoonia*, *34*, 167–266. https://doi.org/10.3767/003158515X688433

Darriba, D., Taboada, G. L., Doallo, R., and Posada, D. 2012. jModelTest 2: More models, new heuristics and high-performance computing. *Nature Methods*, *9*, 772. https://doi.org/10.1038/nmeth.2109

Delgado, A., Garcia-Fernandez, B., Gomez-Cortecero, A., and Dapena, E. 2022. Susceptibility of cider apple accessions to European canker—Comparison between evaluations in field-planted trees and rapid screening tests. *Plants*, *11*, 1145. https://doi.org/10.3390/plants11091145

Dong, J., Shi, H., Wu, Y., Yang, L., Zhu, F., and Ji, Z. 2023. Identification and pathogenicity analysis of *Fusarium* spp. on peach in China. *BMC Microbiology*, *23*, 211. https://doi.org/10.1186/s12866-023-02958-y

Ershad, J. 2022. *Fungi and Fungi-Analogues of Iran.* Iranian Research Institute of Plant Protection, Tehran, Iran. (In Persian).

Esmaeili, N., Mohammadi, H., and Sohrabi, M. 2024. Barberry (*Berberis vulgaris* L.) as an alternative host of grapevine fungal trunk pathogens. *European Journal of Plant Pathology*, *168*, 183–197. https://doi.org/10.1007/s10658-023-02743-7

FAO. 2023. FAOSTAT: Crop production database. Food and Agriculture Organization of the United Nations. Available at: https://www.fao.org/faostat/en/#data/QC (accessed 7 November 2025).

Felsenstein, J. 1985. Confidence limits on phylogenies: An approach using the bootstrap. *Evolution*, *39*, 783–791. https://doi.org/10.1111/j.1558-5646.1985.tb00420.x

Gordon, T. R. 2017. *Fusarium oxysporum* and the *Fusarium* wilt syndrome. *Annual Review of Phytopathology*, *55*, 23–39. https://doi.org/10.1146/annurev-phyto-080615-095919

Guerra, V., Beule, L., Lehtsaar, E., Liao, H. L., and Karlovsky, P. 2020. An improved protocol for DNA extraction from subsoils using phosphate lysis buffer. *Microorganisms*, *8*, 532. https://doi.org/10.3390/microorganisms8040532

Haji Mohammadi, E. 2023. *Investigation of Fungal Root Diseases of Stone Fruit Trees in the Bastam–Shahroud Region.* M.Sc. thesis, Gorgan University of Agricultural Sciences and Natural Resources, Gorgan, Iran. (In Persian).

Hall, T. A. 1999. BioEdit: A user-friendly biological sequence alignment editor and analysis program for Windows 95/98/NT. *Nucleic Acids Symposium Series*, *41*, 95–98.

Hemida, K. A., Ziedan, E. S. H., El-Samman, M. G., Khattab, A. E. N. A., and Mohamed, M. H. 2024. Morphological, molecular biology and pathological characterization of fungi causing root rot on grapevine. *Egyptian Pharmaceutical Journal*, *23*, 368–381.

Houshyar, F., Pouzeshimiyab, B., Nematollahi, S., Kamran, K. V., and Jamshidi, M. 2025. Potential distribution of Fusarium head blight under climate change scenarios in Iran. *Journal of Phytopathology*, *173*, e70034. https://doi.org/10.1111/jph.70034

Hyde, K. D., Dong, Y., Phookamsak, R., Jeewon, R., Bhat, D. J., Jones, E. G., and Perera, R. H. 2020. Fungal diversity notes 1151–1276: Taxonomic and phylogenetic contributions on genera and species of fungal taxa. *Fungal Diversity*, *100*, 5–277. https://doi.org/10.1007/s13225-020-00439-5

Jayarajan, S., and Sharma, R. R. 2020. Postharvest life and quality of 'Snow Queen' nectarine (*Prunus persica* var. *nucipersica*) as influenced by edible coatings during cold storage. *Acta Physiologiae Plantarum*, *42*, 123. https://doi.org/10.1007/s11738-020-03112-1

Katoh, K., and Standley, D. M. 2013. MAFFT multiple sequence alignment software version 7: Improvements in performance and usability. *Molecular Biology and Evolution*, *30*, 772–780. https://doi.org/10.1093/molbev/mst010

Kwak, Y. S., and Weller, D. M. 2013. Take-all of wheat and natural disease suppression: A review. *The Plant Pathology Journal*, *29*, 125–135. https://doi.org/10.5423/PPJ.SI.07.2012.0112

Leslie, J. F., and Summerell, B. A. 2006. *The Fusarium Laboratory Manual*. Blackwell Publishing, Oxford, UK.

Leslie, J. F., and Summerell, B. A. 2016. *Fusarium Laboratory Manual*. Translated by M. Arzanlou, M. Bakhshi, and A. Normani. Age of Life Publications. (In Persian).

Luo, C. X., Schnabel, G., Hu, M., and De Cal, A. 2022. Global distribution and management of peach diseases. *Phytopathology Research*, *4*, 30. https://doi.org/10.1186/s42483-022-00134-0

Ma, X., Miao, J., Wang, J., Han, W., and Sun, Y. 2022. A novel, rapid and simple method for obtaining single-spore isolation of strongly parasitic fungi from diseased cherry leaves. *ScienceAsia*, *48*, 764–768. https://doi.org/10.2306/scienceasia1513-1874.2022.086

Martino, I., Spadaro, D., and Guarnaccia, V. 2025. Fungal trunk pathogens of fruit and nut tree crops: Identification, characterization, detection, and perspectives for a critical global issue. *Plant Disease*, *109*, 1192–1210. https://doi.org/10.1094/PDIS-10-24-2069-FE

Nnadi, N. E., and Carter, D. A. 2021. Climate change and the emergence of fungal pathogens. *PLOS Pathogens*, *17*, e1009503. https://doi.org/10.1371/journal.ppat.1009503

O'Donnell, K., Ward, T. J., Robert, V. A. R. G., Crous, P. W., Geiser, D. M., and Kang, S. 2015. DNA sequence-based identification of *Fusarium*: Current status and future directions. *Phytoparasitica*, *43*, 583–595. https://doi.org/10.1007/s12600-015-0484-z

Paré, L., Banchini, C., Hamel, C., Bernier, L., and Stefani, F. 2022. A simple and low-cost technique to initiate single-spore cultures of arbuscular mycorrhizal fungi using a superabsorbent polymer. *Symbiosis*, *88*, 61–73. https://doi.org/10.1007/s13199-022-00878-5

Pervaiz, Z. H., Contreras, J., Hupp, B. M., Lindenberger, J. H., Chen, D., Zhang, Q., and Saleem, M. 2020. Root microbiome changes with root branching order and root chemistry in peach rhizosphere soil. *Rhizosphere*, *16*, 100249. https://doi.org/10.1016/j.rhisph.2020.100249

Ploetz, R. C. 2015. Fusarium wilt of banana. *Phytopathology*, *105*, 1512–1521. https://doi.org/10.1094/PHYTO-04-15-0101-RVW

Rai, M., and Agarkar, G. 2016. Plant-fungal interactions: What triggers the fungi to switch among lifestyles? *Critical Reviews in Microbiology*, *42*, 428–438. https://doi.org/10.3109/1040841X.2014.958052

Redman, R. S., Dunigan, D. D., and Rodriguez, R. J. 2001. Fungal symbiosis from mutualism to parasitism: Who controls the outcome, host or invader? *New Phytologist*, *151*, 705–716. https://doi.org/10.1046/j.0028-646X.2001.00210.x

Sabahi, F., Banihashemi, Z., Mirtalebi, M., Rep, M., and Cacciola, S. O. 2023. Molecular variability of the *Fusarium solani* species complex associated with Fusarium wilt of melon in Iran. *Journal of Fungi*, *9*, 486. https://doi.org/10.3390/jof9040486

Saremi, H. 2008. *Fusarium: Biology, Ecology and Taxonomy*. Mashhad Academic Jihad Publications, Mashhad, Iran. (In Persian).

Schoch, C. L., Seifert, K. A., Huhndorf, S., Robert, V., Spouge, J. L., Levesque, C. A., and White, M. M. 2012. Nuclear ribosomal internal transcribed spacer (ITS) region as a universal DNA barcode marker for Fungi. *Proceedings of the National Academy of Sciences*, *109*, 6241–6246. https://doi.org/10.1073/pnas.1117018109

Shahrood Agricultural and Natural Resources Research Center. 2022. *Soil and Water Analysis Report of the Bastam Plain Orchards.* Semnan Agricultural and Natural Resources Research and Education Center (AREEO), Iran. (Internal report).

Shen, W., Pan, L., Fu, Y., Suo, Y., Zhang, Y., Liu, H., Su, X., and Zhao, J. 2024. Comparative study on the effectiveness of three inoculation methods for *Valsa sordida* in *Populus alba* var. *pyramidalis*. *Biology*, *13*, 251. https://doi.org/10.3390/biology13040251

Sun, Z. B., Li, S. D., Ren, Q., Xu, J. L., Lu, X., and Sun, M. H. 2020. Biology and applications of *Clonostachys rosea*. *Journal of Applied Microbiology*, *129*, 486–495. https://doi.org/10.1111/jam.14625

Sutton, J. C., Li, D. W., Peng, G., Yu, H., Zhang, P., and Valdebenito-Sanhueza, R. M. 1997. *Gliocladium roseum*, a versatile adversary of *Botrytis cinerea* in crops. *Plant Disease*, *81*, 316–328. https://doi.org/10.1094/PDIS.1997.81.4.316

Tamura, K., Stecher, G., and Kumar, S. 2021. MEGA11: Molecular evolutionary genetics analysis version 11. *Molecular Biology and Evolution*, *38*, 3022–3027. https://doi.org/10.1093/molbev/msab120

van der Merwe, R., Halleen, F., van Dyk, M., Jacobs, V. G., and Mostert, L. 2021. Occurrence of canker and wood rot pathogens on stone fruit propagation material and nursery trees in the Western Cape of South Africa. *Plant Disease*, *105*, 3586–3599. https://doi.org/10.1094/PDIS-10-20-2124-RE

Vu, D., Groenewald, M., De Vries, M., Gehrmann, T., Stielow, B., Eberhardt, U., and Boekhout, T. 2019. Large-scale generation and analysis of filamentous fungal DNA barcodes boosts coverage for kingdom fungi and reveals thresholds for fungal species and higher taxon delimitation. *Studies in Mycology*, *92*, 135–154. https://doi.org/10.1016/j.simyco.2018.05.001

Yuan, G., Czajka, J. J., Dai, Z., Hu, D., Pomraning, K. R., Hofstad, B. A., and Magnuson, J. K. 2023. Rapid and robust squashed spore/colony PCR of industrially important fungi. *Fungal Biology and Biotechnology*, *10*, 15. https://doi.org/10.1186/s40694-023-00163-0

Zakeri, M., and Zare, R. 2013. Diversity of fungal pathogens in nurseries of stone fruit trees in Shahrood region, Iran. *Iranian Journal of Plant Pathology*, *49*, 323–331. (In Persian with English summary).

Zhang, K., Su, Y.-Y., and Cai, L. 2013. An optimized protocol of single spore isolation for fungi. *Cryptogamie, Mycologie*, *34*(4), 349–356. https://doi.org/10.7872/crym.v34.iss4.2013.349

© 2026 by the authors. Licensee SCU, Ahvaz, Iran. This article is an open access article distributed under the terms and conditions of the Creative Commons Attribution-NonCommercial 4.0 International (CC BY-NC 4.0 license) (http://creativecommons.org/licenses/by-nc/4.0/.